

Performance Enhancement of Channel-Phase Precoded Ultra-Wideband (CPP-UWB) Systems by Rake Receivers

Yu-Hao Chang¹, Shang-Ho Tsai², Xiaoli Yu¹ and C.-C. Jay Kuo¹

Ming Hsieh Department of Electrical Engineering, University of Southern California, Los Angeles, CA, USA¹

Department of Electrical and Control Engineering, National Chiao Tung University, Hsinchu, Taiwan²

E-mails: {yuhaocha,xiaoliyu}@usc.edu, shanghot@mail.nctu.edu.tw and cckuo@sipi.usc.edu

Abstract—We propose to use the Rake receiver to improve the system performance by collecting more signal power in an ultra-wideband (UWB) system precoded by the channel phase information, called the CPP-UWB system [1], in this work. The performance of the proposed system is determined by the selected channel taps and the corresponding combining schemes for those Rake fingers. Three combining schemes, *i.e.*, the maximum ratio combining (MRC), the minimized mean square error (MMSE) and the zero-forcing (ZF), are proposed. When the MRC scheme is applied to the Rake receiver with M fingers, M channel taps can be easily found to maximize the averaged signal power at the receiver output by exploiting the property of the channel-phase-precoded channel. It is shown by simulation results that the proposed scheme significantly outperforms the precoding system using one matched filter as proposed in [1].

I. INTRODUCTION

Recently, there is a growing interest in applying the time-reversal prefilter technique (TRP) [2] to UWB transceiver designs. Rather than employing an expensive Rake receiver with tens or even hundreds of fingers to collect sufficient signal power [3], TRP shifts the complexity of multipath combining from the receiver to the transmitter by passing the original transmit signal through a specific prefilter, whose impulse response is the same as the time-reversed UWB channel, so that all the multipath components are combined coherently after certain delay [2]. As a result, a single finger Rake receiver (or the matched filter (MF)) is sufficient to acquire full multipath diversity. This design is attractive to the downlink communication scenario, where the central station (the transmitter) has much more computational power than the mobile unit (the receiver) and a light weight receiver is more favorable.

The full channel knowledge is necessary at the TRP transmitter. However, it is impractical to pass all the channel information from the receiver to the transmitter owing to a great number of channel taps in the UWB channel response. To mitigate this problem, the idea called channel phase precoding (CPP) was proposed lately in [1]. As compared with TRP, the CPP encodes the transmit data with the time-reversed channel phase information alone. Since every phase component corresponds to either $+1$ or -1 , *i.e.*, the sign of channel tap, due to the base band pulse in nature, only one bit is required to describe every phase. Consequently,

the overall feedback overhead in CPP is much lower than that of TRP. The equivalent channel response after phase precoding contains one strong tap since all the channel taps are added constructively. By taking advantage of the concentrated channel power, we may reduce the symbol interval to support a higher data rate communication without suffering much intersymbol interference (ISI) [1].

Nevertheless, the resultant peak signal in CPP is less than that of TRP since not all the channel information is exploited in the precoding process. Since CPP systems rely on the MF filter for symbol decoding, the insufficient peak power can degrade the system performance as well. The situation could be more exacerbated when a serious ISI occurs in some high rate application.

To improve the performance of CPP-UWB systems, it is straight forward to collect more signal power for symbol decoding, *i.e.*, the receiver collects not only the peak but also the off-peak signals by the use of more Rake fingers. The transceiver design of this kind is called CPP-Rake while the previous proposed system in [1] is called CPP-MF in the sequel. Due to its hardware complexity limit, the Rake receiver cannot combine all the channel taps in the resultant channel. Since the decoding performance of the Rake receiver depends on the selected taps and the combining weights for all fingers, both of them should be carefully designed.

In this work, we consider three different weighting design criteria, namely, maximum ratio combining (MRC), minimized mean square error (MMSE) and zero-forcing (ZF). When the data rate is low, *i.e.*, the received signal is ISI free, the MRC scheme can achieve the maximum signal power at the receiver output by synchronizing to those strong taps. Usually, the sorting complexity for a given set is high if the cardinality is large. However, by exploiting the uniqueness of the UWB channel model proposed in [4], we find that the sorting complexity for MRC is indeed very small. On the contrary, when the data rate is high, *i.e.*, the received signal contains ISI, the MRC, which maximizes the signal power, cannot suppress ISI efficiently. Two combining schemes, say, MMSE and ZF, are also developed to improve the system performance by inhibiting or removing ISI at the receiver output. It is pointed out that the reduced-rank multistage Wiener filter (MSWF) [5] can be applied to save the computational power for full-rank MMSE while enjoying a near full-rank performance. Also,

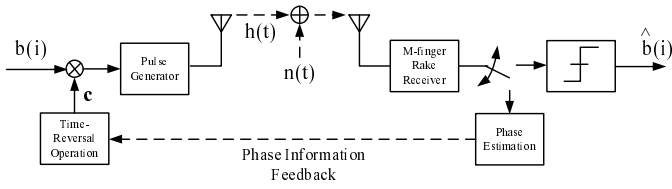


Fig. 1. The block diagram of the proposed UWB system with the channel phase precoding.

canceling all ISI at ZF output may lead to worse performance since ZF suppresses the interference at the cost of reducing the desired signal power.

The rest of the paper is organized as follows. The UWB channel model and the system block diagrams for CPP-Rake is given in Sec. II. The MRC scheme is suitable for a low data rate case and its sorting complexity and system performance are evaluated in Sec. III. For a high data rate case, both MMSE and ZF combining are formulated and derived in Sec. IV. Simulations are conducted to verify three different combining schemes in Sec. V. Finally, concluding remarks are drawn in Sec. VI.

II. SYSTEM MODELS

A carrierless tap-delay-line (TDL) channel model proposed in [4] is adopted in this work and it can be written as

$$h(t) = \sum_{i=0}^{L-1} h_i \delta(t - i\Delta) = \sum_{i=0}^{L-1} p_i \alpha_i \delta(t - i\Delta), \quad (1)$$

where $h_i = p_i \alpha_i$, L is the total number of signal paths, $\delta(x)$ is the Dirac delta function of x , Δ is the multipath resolution, which is set as the time domain pulse width, $p_i \in \{+1, -1\}$ with equal probability is the i th phase component, and the corresponding amplitude component α_i is modeled as a Rayleigh random variable whose probability density function (PDF) is

$$f_{\alpha_i}(x) = \frac{x}{\sigma_i^2} e^{-x^2/2\sigma_i^2}. \quad (2)$$

Furthermore, the power of each tap decreases exponentially with respect to its index, *i.e.*,

$$E\{\alpha_i^2\} = 2\sigma_i^2 = \Omega\gamma^i, \quad (3)$$

where $E\{x\}$ is the expectation of random variable x , Ω is the power of the first tap, and $\gamma = e^{-\Delta/\Gamma}$. In the following context, we assume that the channel is a block fading channel. This means that the channel remains essentially unchanged during the transmission of one package of data symbols and then changes independently from block to block.

The block diagram of the proposed CPP-Rake system is shown in Fig. 1, where the phase information is estimated at the receiver and then sent back to the transmitter for symbol precoding. Generally speaking, the complete channel knowledge is not available at the transmitter due to enormous feedback overhead. Since it takes only one bit to represent every phase component, the phase knowledge can be transmitted through the feedback channel more easily than the amplitude information, which requires several bits to describe its value [1]. Let us consider the case when l first phase components, namely, $[p_0, \dots, p_{l-1}]$, are delivered to the transmitter. The

precoder reverses and normalizes the received data to form the code sequence \mathbf{c} as follows.

$$\mathbf{c} = [c_0, \dots, c_{l-1}]^T = \frac{1}{\sqrt{l}} [p_{l-1}, \dots, p_0]^T,$$

where \mathbf{x}^T and $\|\mathbf{x}\|$ denote the transpose and the 2-norm of vector \mathbf{x} , respectively. The k th antipodal data symbol $b(k)$ with unit power (*i.e.*, $E\{b(k)^2\} = 1$) is encoded by \mathbf{c} and then modulated by pulse waveform $w_s(t)$. As a result, the transmit signal becomes

$$x_s(t) = \sum_{k=-\infty}^{\infty} b(k) \sum_{j=0}^{l-1} c_j w_s(t - kT_s - j\Delta), \quad (4)$$

where the symbol interval $T_s (= N\Delta)$ is assumed to be an integer multiple of the pulse width.

After passing through the channel and antennas at both sides, the received signal is

$$y(t) = \sum_{k=-\infty}^{\infty} b(k) \sum_{i=0}^{L-1} \sum_{j=0}^{l-1} h_i c_j w_r(t - kT_s - (i+j)\Delta) + n(t),$$

where $w_r(t)$ is a unit-power received pulse waveform and $n(t)$ is the zero-mean white Gaussian noise process whose two-sided power spectral density (PSD) is equal to $N_0/2$. Please note that $w_r(t)$ is usually different from $w_s(t)$ due to the antenna effect. Here, it is assumed that $w_r(t)$ is known to the receiver and its pulse width in time domain is roughly equal to Δ . After matching the received pulse waveform and sampling, the discrete received signal $\mathbf{y}(k)$ for $b(k)$ is represented as

$$\begin{aligned} \mathbf{y}(k) &= [y_0(k), \dots, y_{L+l-2}(k)]^T = \mathbf{H}\mathbf{c}b(k) + \mathbf{I}(k) + \mathbf{n}(k), \\ &= \hat{\mathbf{h}}b(k) + \mathbf{I}(k) + \mathbf{n}(k), \end{aligned}$$

where $\hat{\mathbf{h}} = \mathbf{H}\mathbf{c}$ denotes the effective channel response after precoding, \mathbf{H} is the $(L+l-1) \times l$ Toeplitz matrix, where the first column contains $\mathbf{h} = [h_0, \dots, h_{L-1}]^T$ in the first to L th tap and zeros elsewhere, $\mathbf{I}(k)$ is the corresponding intersymbol interference (ISI) vector and $\mathbf{n}(k)$ is the zero-mean noise vector whose covariance matrix equals to $N_0/2\mathbf{I}$. Please note that every element in $\hat{\mathbf{h}} = [\hat{h}_0, \dots, \hat{h}_{L+l-2}]^T$ can be explicitly expressed as

$$\hat{h}_i = \sum_{j=\max\{0, i-l+1\}}^{\min\{i, L-1\}} \frac{1}{\sqrt{l}} p_{l-1-i+j} p_j \alpha_j. \quad (5)$$

for all $i \in \{0, \dots, L+l-2\}$. Among those $L+l-1$ taps in $\hat{\mathbf{h}}$, the greatest signal power occurs at \hat{h}_{l-1} since the first l channel taps are combined coherently.

As compared to the previously proposed CPP-UWB system in [1] where the receiver takes only one sample corresponding to \hat{h}_{l-1} for symbol decoding, we consider the use of M -finger Rake receiver to collect more signal power and hence improve the system performance. Please note that the number of Rake fingers M is much less than the total number of equivalent channel tap in $\hat{\mathbf{h}}$ due to the receiver complexity limitation.

Let us assume the receiver selects M elements out of $\hat{\mathbf{h}}$ for the received signal combining, *i.e.*, $\hat{\mathbf{y}}(k) = [y_{I_0}(k), \dots, y_{I_{M-1}}(k)]^T$, where I_j denotes the j th selected tap index and $I_0 < \dots < I_{M-1}$. If the corresponding $M \times 1$ weighting vector for M -finger is given as $\mathbf{w} = [w_0, \dots, w_{M-1}]^T$, the k th transmitted symbol can be estimated as

$$\hat{b}(k) = \text{sign} \left\{ \mathbf{w}^T \hat{\mathbf{y}}(k) \right\}. \quad (6)$$

III. MRC COMBINING FOR CPP-RAKE SYSTEMS

The performance of CPP-Rake system depends on the selected tap $\{I_0, \dots, I_{M-1}\}$ and the combining vector \mathbf{w} . If the received signal contains no ISI, which corresponds to the low data rate case, a better system performance can be achieved by increasing the output signal power. It is well-known that MRC combining maximizes the signal power for M selected taps [6] and the corresponding weighting vector \mathbf{w}_{mrc} is

$$\mathbf{w}_{mrc} = \frac{1}{\|\hat{\mathbf{h}}_I\|} \hat{\mathbf{h}}_I, \quad (7)$$

where $\hat{\mathbf{h}}_I = [\hat{h}_{I_0}, \dots, \hat{h}_{I_{M-1}}]^T$. The resultant signal power at the MRC output is

$$P_M = \sum_{i=0}^{M-1} E \left\{ \hat{h}_{I_i}^2 \right\}. \quad (8)$$

In order to maximize the output signal power in (8), the receiver has to identify the top M channel taps with highest power in $\hat{\mathbf{h}}$. This requires additional sorting process for $\hat{\mathbf{h}}$, whose complexity is $(L+l-1)\log(L+l-1)$. Since L is usually a large number in UWB channels, sorting is not attractive due to its high computational complexity. It is however that based on the channel model introduced in Sec. II, we find that the sorting complexity can be greatly reduced. Next, we will discuss how to relief the sorting complexity as follows.

A. Channel Taps Selection Algorithm

From (5), we can compute the average power of each tap in $\hat{\mathbf{h}}$. Without going through these detail derivation, we can show that the average power of the k th element in $\hat{\mathbf{h}}$ is given as

$$E \left\{ \hat{h}_i^2 \right\} = \begin{cases} \frac{\Omega}{l} \frac{1-\gamma^{i+1}}{1-\gamma} & \forall 0 \leq i \leq l-2, \\ \left(1 - \frac{\pi}{4}\right) \frac{\Omega(1-\gamma^l)}{l(1-\gamma)} + \frac{\Omega\pi}{4l} \left(\frac{1-\gamma^{l/2}}{1-\gamma^{1/2}}\right)^2 & i = l-1 \\ \frac{\Omega}{l} \frac{1-\gamma^l}{1-\gamma} \gamma^{i-l+1} & \forall l \leq i \leq L-1, \\ \frac{\Omega}{l} \frac{1-\gamma^{L-i+1}}{1-\gamma} \gamma^{i-l+1} & \forall L \leq i \leq L+l-2. \end{cases} \quad (9)$$

It is observed from (9) that the average power of \hat{h}_i , $E\{\hat{h}_i^2\}$, is an increasing function for i less than $l-1$ while it is a decreasing function for i greater or equal to $l-1$. Hence, the remaining sorting process is to figure out the order of any two elements coming from different sets, namely, $\mathbb{S}_1 = \{\hat{h}_i, 0 \leq i \leq l-2\}$ and $\mathbb{S}_2 = \{\hat{h}_i, l-1 \leq i \leq L+l-2\}$. For example, by (9), we can find the upper and lower bounds for each element in \mathbb{S}_1 using elements from \mathbb{S}_2 , *i.e.*,

$$E\{\hat{h}_i^2\} \leq E\{\hat{h}_k^2\} \leq E\{\hat{h}_{i+1}^2\}, \forall k = 0, \dots, l-2, \quad (10)$$

where $\hat{h}_k \in \mathbb{S}_2$ and $\{\hat{h}_i, \hat{h}_{i+1}\} \in \mathbb{S}_2$. Therefore, we can determine the order for all taps in $\hat{\mathbf{h}}^1$. It is worthwhile to comment that the complexity of determining the order of $L+l-1$ elements is low since l is usually a small number in a limited feedback channel. Let $\{o_i, i = 0, \dots, L+l-2\}$ be the indices for the ordered channel taps satisfying

$$E\{\hat{h}_{o_0}^2\} \geq E\{\hat{h}_{o_1}^2\} \geq \dots \geq E\{\hat{h}_{o_{L+l-2}}^2\}. \quad (11)$$

¹We can arbitrarily break the tie condition.

We have the maximum acquired signal power at the MRC Rake output as

$$\max P_M = \sum_{i=0}^{M-1} E \left\{ \hat{h}_{o_i}^2 \right\}. \quad (12)$$

B. Performance Analysis of CPP-Rake with MRC

Here, we demonstrate the signal power capture capability of CPP-Rake receiver with M -finger MRC combining as follows. By (9), the maximum signal power at the output of Rake receiver can be bounded from below as

$$\max P_M = \sum_{i=0}^{M-1} E \left\{ \hat{h}_{o_i}^2 \right\} \geq \sum_{i=l-1}^{l+M-2} E \left\{ \hat{h}_i^2 \right\}. \quad (13)$$

The lower bound developed in (13) is true since we simply combine the first M taps in \mathbb{S}_2 and ignore those strong taps in \mathbb{S}_1 . By substituting (9) into (13) and performing some manipulations, the lower bound is simplified as

$$P_M \geq \sum_{i=l-1}^{l+M-2} E \left\{ \hat{h}_i^2 \right\} = \frac{\Omega\pi}{4l} \left(\frac{1-\gamma^{l/2}}{1-\gamma^{1/2}} \right)^2 + \frac{\Omega(1-\gamma^l)}{l(1-\gamma)} \left(\frac{1-\gamma^M}{1-\gamma} - \frac{\pi}{4} \right). \quad (14)$$

Next, we compare the ratio between the acquired signal power using MRC and the total channel power. The total channel power P_{chl} is calculated as

$$P_{\text{chl}} = \sum_{i=0}^{L-1} E \left\{ h_i^2 \right\} = \sum_{i=0}^{L-1} \Omega\gamma^i = \Omega \frac{1-\gamma^L}{1-\gamma} \approx \frac{\Omega}{1-\gamma}, \quad (15)$$

where we treat $\gamma^L \approx 0$ since L is usually a large number. Let $l = \Gamma\delta/\Delta$, $M = \Gamma\phi/\Delta$ and τ denote the ratio between P_M and P_{chl} . After some manipulations, we can have the lower bound for τ as

$$\tau = \frac{P_M}{P_{\text{chl}}} \geq \frac{\pi\Delta}{4\Gamma\delta} \left(1 - e^{-\delta/2}\right)^2 \frac{1 + e^{-\Delta/2\Gamma}}{1 - e^{-\Delta/2\Gamma}} + \frac{\Delta}{\Gamma\delta} \left(1 - e^{-\delta}\right) \left(\frac{1 - e^{-\phi}}{1 - e^{-\Delta/\Gamma}} - \frac{\pi}{4} \right). \quad (16)$$

Consider the case when the multipath resolution improves, *i.e.*, $\Delta \rightarrow 0$ (or $\frac{\Delta}{\Gamma} \rightarrow 0$), we can have the following approximations as

$$\begin{cases} e^{-\Delta/\Gamma} \approx 1 - \frac{\Delta}{\Gamma}, \\ e^{-\Delta/2\Gamma} \approx 1 - \frac{\Delta}{2\Gamma}. \end{cases} \quad (17)$$

By substituting (17) into (16), we have the lower bound for τ when the pulse width becomes infinitesimal as

$$\lim_{\Delta \rightarrow 0} \tau \geq \frac{\pi}{\delta} \left(1 - e^{-\delta/2}\right)^2 + \frac{\Delta}{\Gamma\delta} \left(1 - e^{-\delta}\right) \left(\frac{\Gamma}{\Delta} \left(1 - e^{-\phi}\right) - \frac{\pi}{4} \right). \quad (18)$$

It is worthwhile to point out that the second terms at the right-hand side of (18) can be viewed as the lower bound for additional power gain coming from employing $(M-1)$ more Rake finger for those off-peak signals in $\hat{\mathbf{h}}$. Both δ and ϕ control the acquired signal power at the MRC output. If δ reduces due to the feedback capacity limit, we may increase the value of ϕ , *i.e.*, use more Rake fingers, to maintain the same signal level. Please note that MRC is only suitable

for the case where interference is small or absent. On the contrary, when the data rate is high, a strong ISI is unavoidable and the performance of MRC degrades as well. Hence, we resort to some complicated combining schemes to combat the interference.

IV. M-FINGER RAKE RECEIVER IN ISI CHANNEL

In this section, we develop two different combining vectors for the CPP-Rake receiver to suppress the interference, namely, the minimum mean square error (MMSE) \mathbf{w}_{mmse} and the zero-forcing \mathbf{w}_{zf} . Please notice that the performance of these two combining schemes depends on the selected channel taps, which could be different based on different design criteria. In order to simplify our discussion, we assume both \mathbf{w}_{mmse} and \mathbf{w}_{zf} pick up the same taps as MRC without developing an individual tap selection algorithm for every combining vector.

A. MMSE Combining

It is easy to show that $\hat{\mathbf{y}}(k)$ contains not only the noise but also the interference coming from $b(k - \lfloor \frac{L+l-1-O_0}{N} \rfloor), \dots, b(k-1)$ and $b(k+1), \dots, b(k + \lfloor \frac{O_{M-1}}{N} \rfloor)$. The corresponding matrix representation for $\hat{\mathbf{y}}(k)$ can be expressed as

$$\hat{\mathbf{y}}(k) = [y_{o_0}(k), \dots, y_{o_{M-1}}(k)]^T = \hat{\mathbf{H}}\mathbf{b}(k) + \hat{\mathbf{n}}(k), \quad (19)$$

where $\mathbf{b}(k) = [b(k - \lfloor \frac{L+l-1-o_0}{N} \rfloor), \dots, b(k + \lfloor \frac{o_{M-1}}{N} \rfloor)]^T$, $\hat{\mathbf{n}}(k) = [n_{o_0}(k), \dots, n_{o_{M-1}}(k)]^T$ and $\hat{\mathbf{H}}$ is the corresponding channel matrix. Based on the system model in (19), the $M \times 1$ weighting vector used to minimize the interference power is constructed as

$$\mathbf{w}_{mmse} = \arg \min_{\mathbf{w}} E \left\{ |b(k) - \mathbf{w}^T \hat{\mathbf{y}}(k)|^2 \right\}. \quad (20)$$

The solution to (20) is the well-known Wiener filter [7] given as

$$\mathbf{w}_{mmse} = \mathbf{R}_{\hat{\mathbf{y}}}^{-1} \hat{\mathbf{p}}, \quad (21)$$

where $\hat{\mathbf{p}} = E\{\hat{\mathbf{y}}(k)b(k)\} = [\hat{h}_{I_0}, \dots, \hat{h}_{I_{M-1}}]^T$ and $\mathbf{R}_{\hat{\mathbf{y}}} = E\{\hat{\mathbf{y}}(k)\hat{\mathbf{y}}(k)^T\} = \hat{\mathbf{H}}\hat{\mathbf{H}}^T + \frac{N_0}{2}\mathbf{I}$.

Please notice that when the dimension of $\mathbf{R}_{\hat{\mathbf{y}}}$ is large, the computational complexity for \mathbf{w}_{mmse} including $\mathbf{R}_{\hat{\mathbf{y}}}^{-1}$ in (21) is high. Rather than computing the full-rank \mathbf{w}_{mmse} directly, we borrow the technique, called reduced-rank multistage Wiener filter (MSWF) [5], to efficiently compute a reduced-rank version of \mathbf{w}_{mmse} . As the simulation results in [5], [8] suggest, a reduced-rank MSWF achieves almost the same system performance as the full-rank MMSE filter while requiring less computational power for the covariance matrix inversion $\mathbf{R}_{\hat{\mathbf{y}}}^{-1}$. Let d denote the rank of the reduced-rank MSWF. The resultant rank- d MSWF is the MMSE filter in the d -dimensional Krylov space spanned by $\mathbf{M}_d = [\hat{\mathbf{p}}, \mathbf{R}_{\hat{\mathbf{y}}}\hat{\mathbf{p}}, \dots, \mathbf{R}_{\hat{\mathbf{y}}}^{d-1}\hat{\mathbf{p}}]$ [8], *i.e.*,

$$\mathbf{w}_{mmse}^{(d)} = \left(\mathbf{M}_d^T \mathbf{R}_{\hat{\mathbf{y}}} \mathbf{M}_d \right)^{-1} \left(\mathbf{M}_d^T \hat{\mathbf{p}} \right). \quad (22)$$

Since the interference power from $b(j) \forall j \neq k$ depends on the relative time distance between $b(j)$ and $b(k)$, not all the interfering symbols contribute the same noise power to $\hat{\mathbf{y}}(k)$. Hence, we may not need to form a full-rank MMSE filter to suppress ISI. As simulation results in Sec. V suggest, a rank-3 MSWF filter provides an almost full-rank performance.

B. Zero-Forcing Combining

The ZF filter, which completely removes the ISI in $\hat{\mathbf{y}}(k)$, is considered in this subsection. Let us first rewrite (19) as

$$\hat{\mathbf{y}}(k) = \hat{\mathbf{p}}b(k) + \hat{\mathbf{H}}_I \mathbf{b}_I(k) + \hat{\mathbf{n}}(k), \quad (23)$$

where $\mathbf{b}_I(k) = [b(k - \lfloor \frac{L+l-1-O_0}{N} \rfloor), \dots, b(k-1), b(k+1), \dots, b(k + \lfloor \frac{O_{M-1}}{N} \rfloor)]^T$ and $\hat{\mathbf{H}}_I$ be the signal matrix formed by removing $\hat{\mathbf{p}}$ in $\hat{\mathbf{H}}$. Here we assume $\hat{\mathbf{H}}_I$ to be a tall matrix, *i.e.*, the number of selected taps is more than the number of interfering symbols, so that \mathbf{w}_{zf} exists. The reason for that will become more clear later in this subsection. The ZF combining design problem can be formulated as

$$\mathbf{w}_{zf} = \arg \max_{\mathbf{w}} E \left\{ |\mathbf{w}^T \hat{\mathbf{p}}|^2 \right\} \quad (24)$$

$$\text{subject to (1) } \mathbf{w}^T \hat{\mathbf{H}}_I = \mathbf{0} \text{ and (2) } \mathbf{w}^T \mathbf{w} = 1,$$

where the second constraint is to limit the power in \mathbf{w}_{zf} to avoid the trivial solution as $\|\mathbf{w}_{zf}\| \rightarrow \infty$. By applying the QR decomposition [9] to the matrix $\hat{\mathbf{H}}_I$, we can have

$$\hat{\mathbf{H}}_I = \mathbf{Q}\mathbf{R}, \quad (25)$$

where \mathbf{Q} is square matrix, which is composed of the M orthonormal basis vectors and \mathbf{R} is a upper triangular matrix, whose dimension is the same as that of $\hat{\mathbf{H}}_I$. Let $\mathbf{Q} = [\mathbf{Q}_1 \mathbf{Q}_2]$, where \mathbf{Q}_1 is the matrix formed by the first $\left(\lfloor \frac{L+l-1-I_0}{N} \rfloor + \lfloor \frac{I_{M-1}}{N} \rfloor \right)$ columns in \mathbf{Q} , *i.e.*, the basis vectors for the interference and \mathbf{Q}_2 is the complementary subspace of \mathbf{Q}_1 . The first constraint in (24) implies that the \mathbf{w}_{zf} must lie in the subspace spanned by \mathbf{Q}_2 . Hence, \mathbf{w}_{zf} can be represented as the linear combination of the columns in \mathbf{Q}_2 , *i.e.*,

$$\mathbf{w} = \mathbf{Q}_2 \mathbf{x}, \quad (26)$$

where \mathbf{x} is the corresponding coefficient vector. Next, by substituting (26) into (24) and performing some manipulations, we can reformulate the filter design problem as

$$\begin{aligned} \mathbf{w}_{zf} &= \mathbf{Q}_2 \mathbf{x}_{zf}, \\ \mathbf{x}_{zf} &= \arg \max_{\mathbf{x}} E \left\{ |\mathbf{x}^T \mathbf{Q}_2^T \hat{\mathbf{p}}|^2 \right\} \text{ subject to } \mathbf{x}^T \mathbf{x} = 1. \end{aligned} \quad (27)$$

The transformed optimization problem in (27) can be easily solved since \mathbf{x}_{zf} is simply the normalized version of vector $\mathbf{Q}_2^T \hat{\mathbf{p}}$. Consequently, we can have \mathbf{w}_{zf} as

$$\mathbf{w}_{zf} = \frac{\mathbf{Q}_2 \mathbf{Q}_2^T \hat{\mathbf{p}}}{\|\mathbf{Q}_2^T \hat{\mathbf{p}}\|}. \quad (28)$$

It is worthwhile to point out that in order to completely remove the interference, the number of Rake finger should be greater or equal to the number of interfered symbols. Otherwise, the dimension of \mathbf{Q}_2 will be zero. In addition, canceling more interfering signals may not guarantee a better system performance. This is because the available signal power at the ZF output goes down due to the reduction of subspace dimension in \mathbf{Q}_2 . We will demonstrate this via simulation in next section.

V. SIMULATION RESULTS

First, we compare the signal power acquired by CPP-Rake and the conventional Rake receiver without precoding. The system parameters are: $L = 120$, $\Delta = 1$ ns, $\Gamma = 20.5$ ns (CM3), $N = 20$ and $l = 10$. The channel power is normalized so that the total power in the channel is unity. The acquired

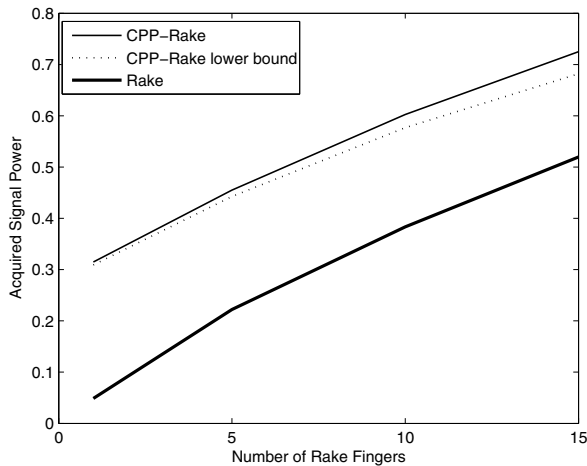


Fig. 2. Comparison of acquired signal power for CPP-Rake and the conventional Rake without precoding.

signal power for different systems is plotted as a function of the number of Rake fingers in Fig. 2, where the result is the average of 1000 independent channel realizations. For performance benchmarking, the performance lower bound for CPP-Rake is also drawn. It is observed that, with the same number of Rake fingers, the CPP-Rake system concentrates more signal power at its output as compared with the conventional Rake receiver. This is because the use of precoding concentrates the signal power spanned in the original channel. It is also suggested by this figure that employing additional Rake fingers is beneficial. For example, four additional Rake fingers can boost more than 50 percent of power gain than the original CPP-MF system. In addition, the lower bound is tight for a small number of Rake fingers and it becomes loose as the number of fingers increases. This is due to the fact that the power gap between taps in \mathbb{S}_1 and \mathbb{S}_2 increases as they are further apart.

Next, we test the capability of interference mitigation using different combining weights, including MRC, MMSE, Rank-3 MSWF and ZF, for the CPP-Rake system with 8 fingers. The other parameters are kept the same as in the previous example. The corresponding bit error rate (BER) curves for different systems are plotted as functions of SNR in Fig. 3. To demonstrate our claim that canceling more interference for \mathbf{w}_{zf} may not provide better performance in Sec. IV, we plot the performance of the ZF combining that only deals with three strongest interfering signals in Fig. 3. Furthermore, the performance curves for CPP-MF in [1] is plotted for comparison. As shown in Fig. 3, a huge performance gain is possible by employing a Rake receiver for phase precoding systems. However, the combining weights for Rake fingers should be carefully design. The MRC scheme fails to suppress enough interference and reaches its BER floor when SNR is greater than 21 dB. The use of Rank-3 MSWF achieves almost the same performance as the full-rank MMSE filter with less computational complexity in filter construction. A better system performance for ZF combining can be achieved

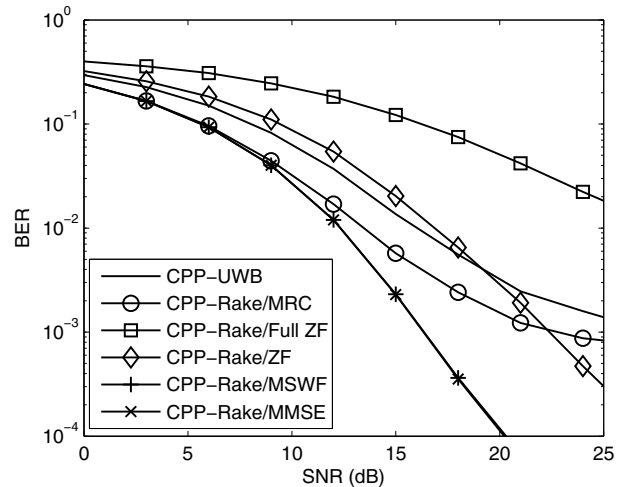


Fig. 3. Comparison of different combining schemes for CPP-Rake systems.

by ignoring some small interfering signals.

VI. CONCLUSION

A Rake receiver was proposed to improve the system performance of CPP-MF in [1] by collecting more signal power in the channel in this work. Three different combining weight vectors for Rake fingers were developed based on different design criteria. In a low data rate scenario, the MRC scheme can be used to achieve the maximum output power. Even though MRC requires an additional sorting process to pick up those strong channel taps, the sorting complexity was shown to be low thanks to the unique channel model. When the data rate is high, more complicated combining schemes such as MMSE and ZF are required to suppress ISI. It was shown by simulation results that the proposed system greatly outperforms the CPP-MF system with a simple matched filter in the receiver.

REFERENCES

- [1] Y.-H. Chang, S.-H. Tsai, X. Yu, and C.-C. J. Kuo, "Ultra-wideband (UWB) transceiver design using channel phase precoding (CPP)," *IEEE Trans. on Signal Processing*, vol. 55, no. 7, pp. 3807–3822, 2007.
- [2] T. Strohmer, M. Emami, J. Hansen, G. Papanicolaous, and A. J. Paulraj, "Application of time-reversal with MMSE equalization to UWB communications," in *Proc. IEEE GLOBECOM'04*, Nov. 2004.
- [3] M. Z. Win and R. A. Scholtz, "On the energy capture of ultrawide bandwidth signals in dense multipath environments," *IEEE Communications Letters*, vol. 2, no. 9, pp. 245–247, Sept. 1998.
- [4] Y.-L. Chao and R. A. Scholtz, "Weighted correlation receivers for ultra-wideband transmitted reference systems," in *Proc. IEEE GLOBECOM'04*, Nov. 2004.
- [5] J. S. Goldstein, I. S. Reed, and L. L. Scharf, "A multistage representation of the Wiener filter based on orthogonal projections," *IEEE Trans. on Information Theory*, vol. 44, no. 7, pp. 2943–2959, Nov. 1998.
- [6] John G. Proakis, *Digital Communications*, McGraw-Hill, 4th edition, 2000.
- [7] S. Haykin, *Adaptive Filter Theory*, Prentice Hall, 4th edition, 2001.
- [8] M. L. Honig and W. Xiao, "Performance of reduced-rank linear interference suppression," *IEEE Trans. on Information Theory*, vol. 47, no. 5, pp. 1928–1946, 2001.
- [9] G. H. Golub and C. F. Van Loan, *Matrix Computations*, Johns Hopkins Press, Baltimore, MD, 3rd edition, 1996.